

Consistency of $f(R) = \sqrt{R^2 - R_0^2}$ Gravity with the Cosmological Observations in Palatini Formalism

M. Sadegh Movahed^{1,2}, Shant Baghram³ and Sohrab Rahvar³

¹*Department of Physics, Shahid Beheshti University, Evin, Tehran 19839, Iran*

²*Institute for Studies in theoretical Physics and Mathematics, P.O.Box 19395-5531, Tehran, Iran*

³*Department of Physics, Sharif University of Technology, P.O.Box 11365-9161, Tehran, Iran*

In this work we study the dynamics of universe in $f(R) = \sqrt{R^2 - R_0^2}$ modified gravity with Palatini formalism. We use data from recent observations as Supernova Type Ia (SNIa) Gold sample and Supernova Legacy Survey (SNLS) data, size of baryonic acoustic peak from Sloan Digital Sky Survey (SDSS), the position of the acoustic peak from the CMB observations and large scale structure formation (LSS) from the 2dFGRS survey to put constraint on the parameters of the model. To check the consistency of this action, we compare the age of old cosmological objects with the age of universe. In the combined analysis with the all the observations, we find the parameters of model as $R_0 = 6.192_{-0.177}^{+0.167} \times H_0^2$ and $\Omega_m = 0.278_{-0.278}^{+0.273}$.
PACS numbers: 04.50.+h, 95.36.+x, 98.80.-k

I. INTRODUCTION

Recent Observations of Supernova type Ia (SNIa) provide the main evidence for the accelerating expansion of the Universe [1,2]. Analysis of SNIa and the Cosmic Microwave Background radiation (CMB) observations indicates that about 70% of the total energy of the Universe is made by the dark energy and the rest of it is in the form of dark matter with a few percent of Baryonic matter [3–5]. The "cosmological constant" is a possible explanation of the present dynamics of the universe [6]. This term in Einstein field equations can be regarded as a fluid with the equation of state of $w = -1$. However, there are two problems with the cosmological constant, namely the *fine-tuning* and the *cosmic coincidence*. In the framework of quantum field theory, the vacuum expectation value is 123 order of magnitude larger than the observed value of 10^{-47} GeV⁴. The absence of a fundamental mechanism which sets the cosmological constant to zero or to a very small value is the cosmological constant problem. The second problem known as the cosmic coincidence, states that why are the energy densities of dark energy and dark matter nearly equal today?

There are various solutions for this problem as the decaying cosmological constant models. A non-dissipative minimally coupled scalar field, so-called Quintessence can play the role of this time varying cosmological constant [7–9]. The ratio of energy density of this field to the matter density in this model increases by the expansion of the universe and after a while dark energy becomes the dominant term of the energy-momentum tensor. One of the features of this model is the variation of equation of state during the expansion of the universe. Various Quintessence models like k-essence [10], tachyonic matter [11], Phantom [12,13] and Chaplygin gas [14] provide various equations of states for the dark energy [13,15–21].

Another approach dealing with this problem is using

the modified gravity by changing the Einstein-Hilbert action. Recently a great attention has been devoted to this era because of the prediction of early and late time accelerations in these models [22]. While it seems that the modified gravity and dark energy models are completely different approaches to explain cosmic acceleration, it is possible to unify them in one formalism [23].

In this work we obtain the dynamics of the modified gravity $f(R) = \sqrt{R^2 - R_0^2}$ in the Palatini formalism [24] and use the cosmological observations as SNIa, SDSS acoustic peck in CMB and structure formation to put constraint on the parameter of the action. In Sec. II we derive the dynamics of Hubble parameter and scale factor in Palatini formalism for general case of $f(R)$ gravity. In Sec. III using action $f(R) = \sqrt{R^2 - R_0^2}$ we obtain the dynamics of universe. In Sec. IV we use the observations from the evolution of background as SNIa, CMB and baryonic acoustic oscillation to constrain the parameters of the model. Sec. V studies constraints from the large scale structure formation and in Sec. VI we compare the age of universe from the model with the age of old cosmological objects. The conclusion is presented in Sec. VII.

II. MODIFIED GRAVITY MODELS IN PALATINI

An alternative approach dealing with the acceleration problem of the Universe is changing the gravity law through the modification of action of gravity by means of using $f(R)$ instead of the Einstein-Hilbert action. For an arbitrary action of the gravity there are two main approaches to extract the field equations. The first one is the so-called metric formalism in which the variation of action is performed with respect to the metric. In the second approach, Palatini formalism, the connection and metric are considered independent of each other and we

have to do variation for those two parameters independently. General form of the action in palatini formalism is :

$$S[f; g, \hat{\Gamma}, \Psi_m] = -\frac{1}{2\kappa} \int d^4x \sqrt{-g} f(R) + S_m[g_{\mu\nu}, \Psi_m], \quad (1)$$

where $\kappa = 8\pi G$ and $S_m[g_{\mu\nu}, \Psi_m]$ is the matter action which depends only on metric $g_{\mu\nu}$ and on the matter fields Ψ_m . $R = R(g, \hat{\Gamma}) = g^{\mu\nu} R_{\mu\nu}(\hat{\Gamma})$ is the generalized Ricci scalar and $R_{\mu\nu}$ is the Ricci tensor of the affine connection which is independent of the metric. Varying the action with respect to the metric results in:

$$f'(R) R_{\mu\nu}(\hat{\Gamma}) - \frac{1}{2} f(R) g_{\mu\nu} = \kappa T_{\mu\nu}, \quad (2)$$

where prime is the differential with respect to Ricci scalar and $T_{\mu\nu}$ is the energy momentum tensor

$$T_{\mu\nu} = \frac{-2}{\sqrt{-g}} \frac{\delta S_m}{\delta g^{\mu\nu}}. \quad (3)$$

Varying the action with respect to the connection and after contraction gives us the equation that determines the generalized connection as:

$$\hat{\nabla}_\alpha [f'(R) \sqrt{-g} g^{\mu\nu}] = 0, \quad (4)$$

where $\hat{\nabla}$ is the covariant derivative with respect to the affine connection. We can see that the connections are the Christoffel symbols of the new metric $h_{\mu\nu}$ where it is conformally related to the original one via the $h_{\mu\nu} = f'(R) g_{\mu\nu}$.

Equation (2) shows that in contrast to the metric variation approach, the field equations are second order in this formalism which seems more intuitive to have second order equations instead of fourth order. On the other hand fourth order differential equations have the instability problem [28]. We use FRW metric for universes as follows

$$ds^2 = -dt^2 + a(t)^2 \delta_{ij} dx^i dx^j \quad (5)$$

and assume universe is filled with perfect fluid with the energy-momentum tensor of $T_\mu^\nu = \text{diag}(-\rho, p, p, p)$, taking the trace of equation (2) gives,

$$Rf'(R) - 2f(R) = \kappa T, \quad (6)$$

where $T = g^{\mu\nu} T_{\mu\nu} = -\rho + 3p$. Using Generalized Einstein equation (2) and FRW metric we obtain generalized FRW equation as [29]:

$$\left(H + \frac{1}{2} \frac{\dot{f}'}{f'}\right)^2 = \frac{1}{6} \frac{\kappa(\rho + 3p)}{f'} - \frac{1}{6} \frac{f}{f'}. \quad (7)$$

For the cosmic fluid with the equation of state of $p = p(\rho)$, using the continuity equation and the trace of field

equation we can express the time derivative of Ricci scalar as:

$$\dot{R} = +3H \frac{(1-3p')(\rho+p)}{Rf'' - f'(R)}. \quad (8)$$

Using equation (6) we obtain the density of matter in terms of Ricci scalar as:

$$\kappa\rho = \frac{2f - Rf'}{1 - 3\omega}, \quad (9)$$

where $\omega = p/\rho$. Substituting (9) in (7) we obtain the dynamics of universe in terms of Ricci scalar:

$$H^2 = \frac{1}{6(1-3\omega)f'} \frac{3(1+\omega)f - (1+3\omega)Rf'}{\left[1 + \frac{3}{2}(1+\omega) \frac{f'(Rf'-2f)}{f'(Rf''-f')}\right]^2}. \quad (10)$$

On the other hand using equation (6) and continuity equation, the scale factor can be obtained in terms of Ricci scalar

$$a = \left[\frac{1}{\kappa\rho_0(1-3\omega)} (2f - Rf') \right]^{-\frac{1}{3(1+\omega)}}, \quad (11)$$

where ρ_0 is the energy density at the present time and we set $a_0 = 1$. Now for a modified gravity action, omitting Ricci scalar in favor of the scale factor between equations (10) and (11) we can obtain the dynamics of universe (i.e. $H = H(a)$). For the matter dominant epoch $\omega = 0$, these equations reduce to:

$$H^2 = \frac{1}{6f'} \frac{3f - Rf'}{\left[1 + \frac{3}{2} \frac{f''(Rf'-2f)}{f'(Rf''-f')}\right]^2} \quad (12)$$

$$a = \left[\frac{1}{\kappa\rho_0} (2f - Rf') \right]^{-\frac{1}{3}} \quad (13)$$

III. MODIFIED GRAVITY WITH THE ACTION OF $F(R) = \sqrt{R^2 - R_0^2}$

In this section our aim is to apply the action of $f(R) = \sqrt{R^2 - R_0^2}$ in equations (10) and (11) to obtain the dynamics of universe. For simplicity we use dimensionless parameters in our calculation defined by

$$f(R) = H_0^2 \sqrt{X^2 - X_0^2} \quad (14)$$

in which H_0 is the Hubble parameter at the present time and $X \equiv \frac{R}{H_0^2}$ and $X_0 \equiv \frac{R_0}{H_0^2}$. For convenience we can write the action and its derivatives as:

$$f(R) = H_0^2 F(X) \quad (15)$$

$$f'(R) = F'(X) \quad (16)$$

$$f''(R) = \frac{F''(X)}{H_0^2} \quad (17)$$

where derivative at the right hand side of equations is with respect to X (i.e. $' = \frac{d}{dX}$). We can write (12) with new parameter of X as:

$$\mathcal{H}(X) = \frac{1}{6F'} \frac{3F - XF'}{\left(1 + \frac{3}{2} \frac{F''(XF' - 2F)}{F'(XF'' - F')}\right)^2}, \quad (18)$$

where $\mathcal{H}(X) = H^2/H_0^2$ and H_0 is the Hubble parameter at the present time. Using the definition of $\Omega_m(X) \equiv \kappa\rho_m/(3H^2)$ from equation (9) we can obtain $\Omega_m(X)$ in terms X as:

$$\Omega_m(X) = \frac{2F - XF'}{3}. \quad (19)$$

We use $\Omega_m(X) = \Omega_m a^{-3}$ (where $\Omega_m \equiv \Omega_m^{(0)}$) and substitute F in terms of X from (14) to obtain scale factor in terms of X as:

$$a = \left[\frac{1}{3\Omega_m} \left(\frac{X^2 - 2X_0^2}{\sqrt{X^2 - X_0^2}} \right) \right]^{-1/3}, \quad (20)$$

where to have positive scale factor, X should change in the range of $X \geq \sqrt{2}X_0$. It should be noted that this model has only one free parameter of X_0 . X_p represents the value of X at the present time and from (18) we can find X_p in terms of X_0 . On the other hand substituting $X_p = g(X_0)$ in (19) we will have direct relation between X_0 and Ω_m . So knowing X_0 from observation one can calculate also Ω_m .

In the next section we will compare observations with the dynamics provided by this model in the matter dominant epoch. However we can see how the universe expands at the radiation dominant epoch. We set $p = 1/3\rho$ which implies traceless energy momentum tensor and using our proposed action in equation (6), we get a constant Ricci scalar of $R = \sqrt{2}R_0$ for this area. Substituting this constant curvature in equation (7) we have:

$$H^2 = \frac{\kappa}{3\sqrt{2}}\rho - \frac{1}{6\sqrt{2}}R_0. \quad (21)$$

Since R_0 is in the order of H_0^2 (see [24]), for the early universe we can ignore second term at the right hand side of this equation which results the scale factor to increase as $a \propto t^{1/2}$.

IV. OBSERVATIONAL CONSTRAINTS FROM THE BACKGROUND EVOLUTION

In this section we compare the new SNIa Gold sample and supernova Legacy Survey data, the location of baryonic acoustic oscillation peak from the SDSS and the location of acoustic peak from the CMB observation to constrain the parameters of the model. We choose various priors applied in the this analysis as shown in Table I

TABLE I. Different priors on the parameter space, used in the likelihood analysis.

Parameter	Prior	
Ω_{tot}	1.00	Fixed
$\Omega_b h^2$	0.020 ± 0.005	Top hat (BBN) [25]
h	—	Free [26,27]
w	0	Fixed

A. Examining the Model by Supernova Type Ia: Gold Sample

The Supernova Type Ia experiments provided the main evidence for the present acceleration of the universe. Since 1995 two teams of the *High-Z Supernova Search* and the *Supernova Cosmology Project* have discovered several type Ia supernovas at the high redshifts [17,30]. Riess et al.(2004) announced the discovery of 16 type Ia supernova with the Hubble Space Telescope. This new sample includes 6 of the 7 most distant ($z > 1.25$) type Ia supernovas. They determined the luminosity distance of these supernovas and with the previously reported algorithms, obtained a uniform 157 Gold sample of type Ia supernovas [31–33]. Recently a new data set of Gold sample with smaller systematic error containing 156 Supernova Ia has been released [34]. In this work we use this data set as new Gold sample SNIa.

More recently, the SNLS collaboration released the first year data of its planned five-year Supernova Legacy Survey [35]. An important aspect to be emphasized on the SNLS data is that they seem to be in a better agreement with WMAP results than the Gold sample [36].

We calculate the apparent magnitude from the $f(R)$ modified gravity and compare with new SNIa Gold sample and SNLS data set. The supernova measured apparent magnitude m includes reddening, K correction, etc, which here all these effect have been removed. The apparent magnitude is related to the (dimensionless) luminosity distance, D_L , of an object at redshift z through:

$$m = \mathcal{M} + 5 \log D_L(z; X_0), \quad (22)$$

where

$$D_L(z; X_0) = (1+z) \int_0^z \frac{dz' H_0}{H(z')} \quad (23)$$

Also

$$\mathcal{M} = M + 5 \log \left(\frac{c/H_0}{1 \text{ Mpc}} \right) + 25. \quad (24)$$

where M is the absolute magnitude. The distance modulus, μ , is defined as:

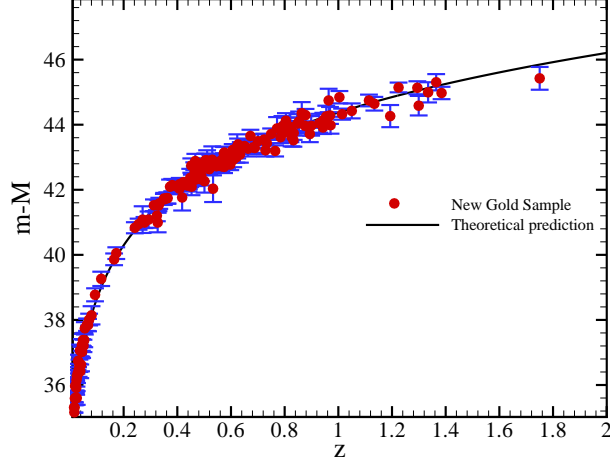


FIG. 1. Distance modulus of the SNIa new Gold sample in terms of redshift. Solid line shows the best fit values with the corresponding parameters of $h = 0.63$, $\Omega_m = 0.276^{+0.376}_{-0.240}$, $X_0 = 6.207^{+0.230}_{-0.147}$ in 1σ level of confidence with $\chi^2_{min}/N_{d.o.f} = 0.912$ for $f(R)$ model.

$$\mu \equiv m - M = 5 \log D_L(z; X_0) + 5 \log \left(\frac{c/H_0}{1 \text{ Mpc}} \right) + 25, \quad (25)$$

or

$$\mu = 5 \log D_L(z; X_0) + \bar{M}. \quad (26)$$

To compare the theoretical results with the observational data, we calculate theoretical distance modulus. Distance modulus can be written in terms of new parameter X as:

$$D_L = \frac{1}{3} \frac{(XF' - 2F)^{(\frac{1}{3})}}{(3\Omega_m)^{\frac{2}{3}}} \int_{X_p}^X \frac{XF'' - F'}{(XF' - 2F)^{\frac{2}{3}}} \frac{dX}{\mathcal{H}(X)}. \quad (27)$$

To put constraint on the model parameter, the first step is to compute the quality of the fitting through the least squared fitting quantity χ^2 defined by:

$$\chi^2(\bar{M}, X_0) = \sum_i \frac{[\mu_{obs}(z_i) - \mu_{th}(z_i; X_0, \bar{M})]^2}{\sigma_i^2}, \quad (28)$$

where σ_i is all of observational uncertainty in the distance modulus. To constrain the parameters of model, we use the Likelihood statistical analysis:

$$\mathcal{L}(\bar{M}, X_0) = \mathcal{N} e^{-\chi^2(\bar{M}, X_0)/2}, \quad (29)$$

where \mathcal{N} is a normalization factor. The parameter \bar{M} is a nuisance parameter and should be marginalized (integrated out) leading to a new $\bar{\chi}^2$ defined as:

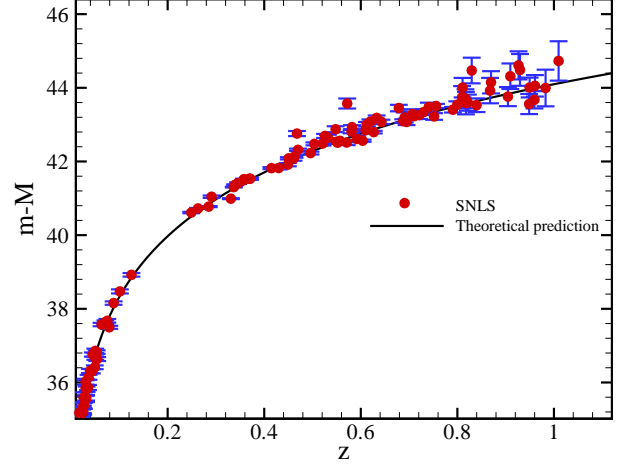


FIG. 2. Distance modulus of the SNLS supernova data in terms of redshift. Solid line shows the best fit values with the corresponding parameters of $h = 0.70$, $\Omega_m = 0.246^{+0.164}_{-0.164}$ and $X_0 = 6.484^{+0.099}_{-0.099}$ in 1σ level of confidence with $\chi^2_{min}/N_{d.o.f} = 11.766$ for $f(R)$ model.

$$\bar{\chi}^2 = -2 \ln \int_{-\infty}^{+\infty} e^{-\chi^2/2} d\bar{M}. \quad (30)$$

Using equations (28) and (30), we find:

$$\bar{\chi}^2(X_0) = \chi^2(\bar{M} = 0, X_0) - \frac{B(X_0)^2}{C} + \ln(C/2\pi), \quad (31)$$

where

$$B(X_0) = \sum_i \frac{[\mu_{obs}(z_i) - \mu_{th}(z_i; X_0, \bar{M} = 0)]}{\sigma_i^2}, \quad (32)$$

and

$$C = \sum_i \frac{1}{\sigma_i^2}. \quad (33)$$

Equivalent to marginalization is the minimization with respect to \bar{M} . One can show that $\bar{\chi}^2$ can be expanded in terms of \bar{M} as [37]:

$$\chi^2_{\text{SNIa}}(X_0) = \chi^2(\bar{M} = 0, X_0) - 2\bar{M}B + \bar{M}^2C, \quad (34)$$

which has a minimum for $\bar{M} = B/C$:

$$\chi^2_{\text{SNIa}}(X_0) = \chi^2(\bar{M} = 0, X_0) - \frac{B(X_0)^2}{C}. \quad (35)$$

Using equation (35) we can find the best fit values of model parameters, minimizing $\chi^2_{\text{SNIa}}(X_0)$. Using new Gold sample SNIa, the best fit values for the free parameter of the model is $X_0 = 6.207^{+0.230}_{-0.147}$ states

$\Omega_m = 0.276^{+0.376}_{-0.240}$, with $\chi_{min}^2/N_{d.o.f} = 0.912$ at 1σ level of confidence. The corresponding value for the Hubble parameter at the minimized χ^2 is $h = 0.64$ and since we have already marginalized over this parameter we do not assign an error bar for it. The best fit values for the parameters of model by using SNLS supernova data is $X_0 = 6.484^{+0.099}_{-0.099}$ indicates $\Omega_m = 0.246^{+0.164}_{-0.164}$ with $\chi_{min}^2/N_{d.o.f} = 11.766$ at 1σ level of confidence. Figures 1 and 2 show the comparison of the theoretical prediction of distance modulus by using the best fit value of X_0 and observational values from new Gold sample and SNLS supernova Ia, respectively. In figures 5, 6, relative likelihood for X_0 are indicated. We report the best value of X_0 at 1 and 2- σ confidence level and other derived parameters in table II.

B. CMBR Shift parameter

Before last scattering, the photons and baryons are tightly coupled by Compton scattering and behave as a fluid. The oscillations of this fluid, occurring as a result of the balance between the gravitational interactions and the photon pressure, lead to the familiar spectrum of peaks and troughs in the averaged temperature anisotropy spectrum which we measure today. The odd peaks correspond to maximum compression of the fluid, the even ones to rarefaction [38]. In an idealized model of the fluid, there is an analytic relation for the location of the m -th peak: $l_m \approx ml_A$ [39,40] where l_A is the acoustic scale which may be calculated analytically and depends on both pre- and post-recombination physics as well as the geometry of the universe. The acoustic scale corresponds to the Jeans length of photon-baryon structures at the last scattering surface some ~ 379 Kyr after the Big Bang [5]. The apparent angular size of acoustic peak can be obtained by dividing the comoving size of sound horizon at the decoupling epoch $r_s(z_{dec})$ by the comoving distance of observer to the last scattering surface $r(z_{dec})$:

$$\theta_A = \frac{\pi}{l_A} \equiv \frac{r_s(z_{dec})}{r(z_{dec})}. \quad (36)$$

The size of sound horizon at the numerator of equation (36) corresponds to the distance that a perturbation of pressure can travel from the beginning of universe up to the last scattering surface and is given by:

$$r_s(z_{dec}) = \int_{z_{dec}}^{\infty} \frac{v_s(z') dz'}{H(z')/H_0} \quad (37)$$

where $v_s(z)^{-2} = 3 + 9/4 \times \rho_b(z)/\rho_{rad}(z)$ is the sound velocity in the unit of speed of light from the big bang up to the last scattering surface [19,39] and the redshift of the last scattering surface, z_{dec} , is given by [39]:

$$\begin{aligned} z_{dec} &= 1048 [1 + 0.00124(\omega_b)^{-0.738}] [1 + g_1(\omega_m)^{g_2}], \\ g_1 &= 0.0783(\omega_b)^{-0.238} [1 + 39.5(\omega_b)^{0.763}]^{-1}, \\ g_2 &= 0.560 [1 + 21.1(\omega_b)^{1.81}]^{-1}, \end{aligned} \quad (38)$$

where $\omega_m \equiv \Omega_m h^2$ and $\omega_b \equiv \Omega_b h^2$. Changing the parameters of the model can change the size of apparent acoustic peak and subsequently the position of $l_A \equiv \pi/\theta_A$ in the power spectrum of temperature fluctuations on CMB. The simple relation $l_m \approx ml_A$ however does not hold very well for the first peak although it is better for higher peaks [2]. Driving effects from the decay of the gravitational potential as well as contributions from the Doppler shift of the oscillating fluid introduce a shift in the spectrum. A good parameterization for the location of the peaks and troughs is given by [40,41]

$$l_m = l_A(m - \phi_m) \quad (39)$$

where ϕ_m is phase shift determined predominantly by pre-recombination physics, and are independent of the geometry of the Universe. Instead of the peak locations of power spectrum of CMB, one can use another model independent parameter which is so-called shift parameter \mathcal{R} as:

$$\mathcal{R} \propto \frac{l_1^{flat}}{l_1} \quad (40)$$

where l_1^{flat} corresponds to flat pure-CDM model with $\Omega_m = 1.0$ and the same ω_m and ω_b as the original model. The location of first acoustic peak can be determined in model by equation (39) with $\phi_1(\omega_m, \omega_b) \simeq 0.27$ [40,41]. It is easily shown that shift parameter is as follows [42]:

$$\mathcal{R} = \sqrt{\Omega_m} \frac{D_L(z_{dec}; X_0)}{(1 + z_{dec})} \quad (41)$$

In writing the shift parameter in this form we have implicitly assumed that photons follow geodesics determined by the Levi-Civita connection. Furthermore, in order to use the shift parameter, the evolution of the universe is considered in such a way that at the decoupling we have standard matter dominated behavior. Since we do not have an explicit expression for the Hubble parameters in terms of redshift, it is useful to rewrite the shift parameter in terms of dimensionless parameter X as follows:

$$\begin{aligned} \mathcal{R} &= \sqrt{\Omega_m H_0^2} \int_0^{z_{dec}} \frac{dz}{H(z)} \\ &= \sqrt{\Omega_m H_0^2} \int_{R_{dec}}^{R_p} \frac{a'(R)}{a^2(R)} \frac{dR}{H(R)} \\ &= \frac{\Omega_m^{\frac{1}{6}}}{3^{\frac{4}{3}}} \int_{X_p}^{X_{dec}} \frac{F' - XF''}{(2F - XF')^{\frac{2}{3}} \mathcal{H}(X)} dX \end{aligned} \quad (42)$$

The observational results of CMB experiments correspond to a shift parameter of $\mathcal{R} = 1.716 \pm 0.062$ (given by

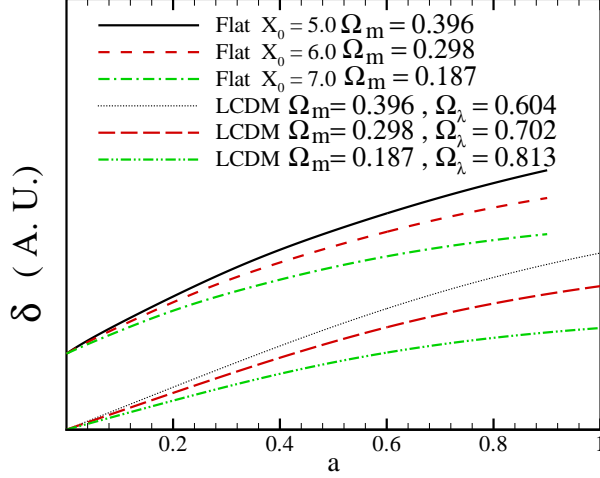


FIG. 3. Evolution of density contrast in the $f(R)$ gravity model versus redshift for different values of X_0 . For comparison we plot δ for Λ CDM with the same value of Ω_m . (A.U. stands for arbitrary unit)

WMAP, CBI, ACBAR) [5,43]. One of the advantages of using the parameter \mathcal{R} is that it is independent of Hubble constant. In order to put constraint on the model from CMB, we compare the observed shift parameter with that of model using likelihood statistic as [42]:

$$\mathcal{L} \sim e^{-\chi_{\text{CMB}}^2/2} \quad (43)$$

where

$$\chi_{\text{CMB}}^2 = \frac{[\mathcal{R}_{\text{obs}} - \mathcal{R}_{\text{the}}]^2}{\sigma_{\text{CMB}}^2} \quad (44)$$

C. Baryon Acoustic Oscillations

The large scale correlation function measured from 46,748 *Luminous Red Galaxies* (LRG) spectroscopic sample of the SDSS (Sloan Digital Sky Survey) includes a clear peak at about $100 \text{ Mpc } h^{-1}$ [44]. This peak was identified with the expanding spherical wave of baryonic perturbations originating from acoustic oscillations at recombination. The comoving scale of this shell at recombination is about 150 Mpc in radius. A dimensionless and independent of H_0 of this observation is:

$$\mathcal{A} = \sqrt{\Omega_m} \left[\frac{H_0 D_L^2(z_{\text{sdss}}; X_0)}{H(z_{\text{sdss}}; X_0) z_{\text{sdss}}^2 (1 + z_{\text{sdss}})^2} \right]^{1/3} \quad (45)$$

or

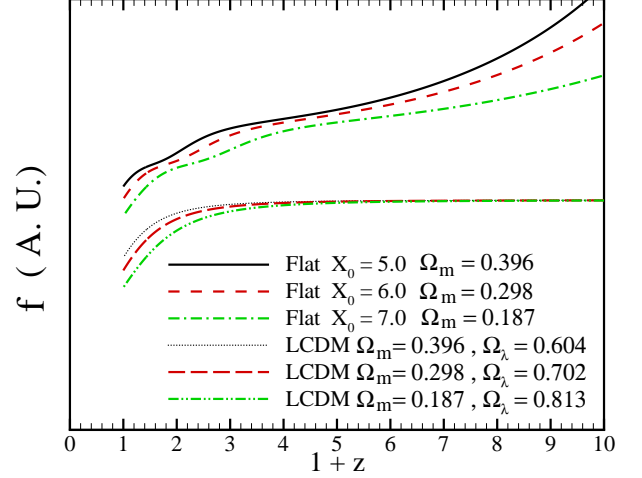


FIG. 4. Growth index versus redshift for different values of X_0 . To make sense we plot f for Λ CDM with the same Ω_m .

$$\mathcal{A} = \sqrt{\Omega_m} \mathcal{H}(X)^{-\frac{1}{3}} \left[\frac{1}{z_{\text{sdss}}} \int_0^{z_{\text{sdss}}} \frac{dz}{\mathcal{H}(X)} \right]^{\frac{2}{3}} \quad (46)$$

we can write the above dimensionless quantity in term of our model parameter as:

$$\mathcal{A} = \sqrt{\Omega_m} \mathcal{H}(X)^{-\frac{1}{3}} \times \left[\frac{(3\Omega_m)^{-\frac{1}{3}}}{3z_{\text{sdss}}} \int_{X_p}^{X_{\text{sdss}}} \frac{(F' - XF'')dX}{\mathcal{H}(X)(2F - XF')^{2/3}} \right]^{\frac{2}{3}} \quad (47)$$

We can put the robust constraint on the $f(R)$ modified gravity model using the value of $\mathcal{A} = 0.469 \pm 0.017$ from the LRG observation at $z_{\text{sdss}} = 0.35$ [44]. This observation permits the addition of one more term in the χ^2 of equations (35) and (44) to be minimized with respect to $H(z)$ model parameters. This term is:

$$\chi_{\text{SDSS}}^2 = \frac{[\mathcal{A}_{\text{obs}} - \mathcal{A}_{\text{the}}]^2}{\sigma_{\text{SDSS}}^2} \quad (48)$$

This is the third observational constraint for our analysis.

D. Combined analysis: SNIa+CMB+SDSS

In this section we combine SNIa data (from SNIa new Gold sample and SNLS), CMB data from the WMAP with recently observed baryonic peak from the SDSS to constrain the parameter of modified gravity model by minimizing the combined $\chi^2 = \chi_{\text{SNIa}}^2 + \chi_{\text{CMB}}^2 + \chi_{\text{SDSS}}^2$ [45].

The best values of the model parameters from the fitting with the corresponding error bars from the likelihood

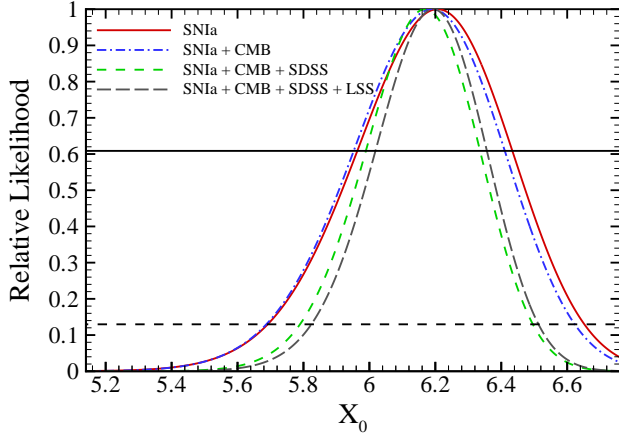


FIG. 5. Marginalized likelihood functions of $f(R)$ modified gravity model free parameter, X_0 . The solid line corresponds to the likelihood function of fitting the model with SNIa data (new Gold sample), the dashdot line with the joint SNIa+CMB+SDSS data and dashed line corresponds to SNIa+CMB+SDSS+LSS. The intersections of the curves with the horizontal solid and dashed lines give the bounds with 1σ and 2σ level of confidence respectively.

function marginalizing over the Hubble parameter in the multidimensional parameter space are: $X_0 = 6.169^{+0.170}_{-0.184}$ corresponds to $\Omega_m = 0.281^{+0.277}_{-0.281}$ at 1σ confidence level with $\chi^2_{min}/N_{d.o.f} = 0.902$. The Hubble parameter corresponding to the minimum value of χ^2 is $h = 0.63$. Here we obtain an age of $14.56^{+0.29}_{-0.28}$ Gyr for the universe. Using the SNLS data, the best fit values of model parameter is: $X_0 = 6.428^{+0.00}_{-0.092}$ states $\Omega_m = 0.252^{+0.148}_{-0.152}$ at 1σ confidence level with $\chi^2_{min}/N_{d.o.f} = 11.582$. Table II indicates the best fit values for the cosmological parameters with one and two σ level of confidence. Relative likelihood analysis for X_0 using CMB and SDSS observations are shown in figures 5 and 6.

V. CONSTRAINTS BY LARGE SCALE STRUCTURE

So far we have only considered observational results related to the background evolution. In this section using the linear approximation of structure formation we obtain the growth index of structures and compare it with the result of observations by the 2-degree Field Galaxy Redshift Survey (2dFGRS). The continuity and modified Poisson equations for the density contrast $\delta = \delta\rho/\bar{\rho}$ in the cosmic fluid provide the evolution of density contrast in the linear approximation (i.e. $\delta \ll 1$) [46,47] as:

$$\ddot{\delta} + 2\frac{\dot{a}}{a}\dot{\delta} - [v_s^2\nabla^2 + 4\pi G\rho]\delta = 0, \quad (49)$$

the dot denotes the derivative with respect to time. The effect of modified gravity in the evolution of the struc-

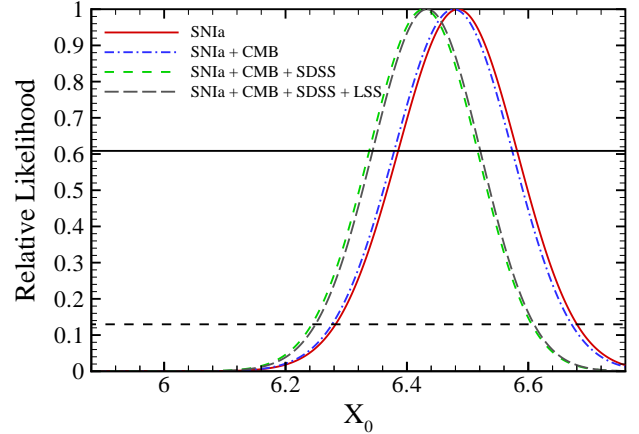


FIG. 6. Marginalized likelihood functions of $f(R)$ modified gravity model free parameter, X_0 . The solid line corresponds to the likelihood function of fitting the model with SNIa data (SNLS), the dashdot line with the joint SNIa+CMB+SDSS data and dashed line corresponds to SNIa+CMB+SDSS+LSS. The intersections of the curves with the horizontal solid and dashed lines give the bounds with 1σ and 2σ level of confidence respectively.

tures in this equation enters through its influence on the expansion rate.

The validity of this linear Newtonian approach is restricted to perturbations on the sub-horizon scales but large enough where structure formation is still in the linear regime [46–48]. For the perturbations larger than the Jeans length, $\lambda_J = \pi^{1/2}v_s/\sqrt{G\rho}$, equation (49) for cold dark matter (CDM) reduces to:

$$\ddot{\delta} + 2\frac{\dot{a}}{a}\dot{\delta} - 4\pi G\rho\delta = 0. \quad (50)$$

The equation for the evolution of density contrast can be rewritten in terms of the scale factor as:

$$\frac{d^2\delta}{da^2} + \frac{d\delta}{da} \left[\frac{\ddot{a}}{\dot{a}^2} + \frac{2H}{\dot{a}} \right] - \frac{3H_0^2}{2\dot{a}^2 a^3} \Omega_m \delta = 0. \quad (51)$$

In order to use the constraint from large scale structure we should rewrite above equation in terms of X . So we have

$$\begin{aligned} \dot{a} &= aH(X), \\ \ddot{a} &= aH^2(X) + a^2H(X)H'(X)\frac{dX}{da}. \end{aligned} \quad (52)$$

Using equation (52), equation (51) becomes:

$$\frac{d^2\delta}{da^2} + \frac{d\delta}{da} \left[\frac{3}{a} + \frac{H'(X)}{H(X)} \frac{dX}{da} \right] - \frac{3\Omega_m}{2H^2(X)a^5} \delta = 0 \quad (53)$$

Numerical solution of equation (53) in FRW universe for the two cases of $f(R)$ gravity and Λ CDM model with the same matter density content is compared in Figure (3).

In the linear perturbation theory, the peculiar velocity field \mathbf{v} is determined by the density contrast [46,49] as:

$$\mathbf{v}(\mathbf{x}) = H_0 \frac{f}{4\pi} \int \delta(\mathbf{y}) \frac{\mathbf{x} - \mathbf{y}}{|\mathbf{x} - \mathbf{y}|^3} d^3\mathbf{y}, \quad (54)$$

where the growth index f is defined by:

$$f = \frac{d \ln \delta}{d \ln a}, \quad (55)$$

and it is proportional to the ratio of the second term of equation (50) (friction) to the third (Poisson) term.

We use the evolution of the density contrast δ to compute the growth index of structure f , which is an important quantity for the interpretation of peculiar velocities of galaxies [49,50]. Replacing the density contrast with the growth index in equation (51) results in the evolution of growth index as:

$$\frac{df}{d \ln a} = \frac{3H_0^2}{2\dot{a}^2 a} \Omega_m - f^2 - f \left[1 + \frac{\ddot{a}}{aH^2} \right]. \quad (56)$$

The above equation in terms of dimensionless quantity is:

$$\frac{df}{d \ln a} = \frac{3\Omega_m}{2a\mathcal{H}^2(X)} - f^2 - f \left[2 + \frac{a\mathcal{H}'(X)}{\mathcal{H}(X)} \frac{dX}{da} \right]. \quad (57)$$

Figure (4) shows the numerical solution of equation (57) in terms of redshift. As we expect increasing X_0 causes decreasing Ω_m from best fit and a decreasing in the evolution of density contrast versus scale factor and growth index in the small redshifts. This behavior is the same as what happens in the Λ CDM model.

To put constraint on the model using large structure formation, we rely to the observation of 220,000 galaxies with the 2dFGRS experiment provides the numerical value of growth index [44]. By measurements of two-point correlation function, the 2dFGRS team reported the redshift distortion parameter of $\beta = f/b = 0.49 \pm 0.09$ at $z = 0.15$, where b is the bias parameter describing the difference in the distribution of galaxies and their masses. Verde et al. (2003) used the bispectrum of 2dFGRS galaxies [51,52] and obtained $b_{verde} = 1.04 \pm 0.11$ which gave $f = 0.51 \pm 0.10$. Now we fit the growth index at the present time derived from the equation (57) with the observational value. This fitting gives a less constraint to the parameters of the model, so in order to have a better confinement of the parameters, we combine this fitting with those of SNIa+CMB+SDSS which have been discussed in the previous section. We perform the least square fitting by minimizing $\chi^2 = \chi_{\text{SNIa}}^2 + \chi_{\text{CMB}}^2 + \chi_{\text{SDSS}}^2 + \chi_{\text{LSS}}^2$, where

$$\chi_{\text{LSS}}^2 = \frac{[f_{\text{obs}}(z = 0.15) - f_{\text{th}}(z = 0.15; X_0)]^2}{\sigma_{f_{\text{obs}}}^2} \quad (58)$$

The best fit value with the corresponding error bar for the X_0 by using new Gold sample data is: $X_0 =$

$6.192_{-0.177}^{+0.167}$ provides $\Omega_m = 0.278_{0.278}^{+0.273}$ at 1σ confidence level with $\chi_{\text{min}}^2/N_{\text{d.o.f}} = 0.900$. Using the SNLS supernova data, the best fit value for model parameter is: $X_0 = 6.433_{-0.091}^{+0.089}$ gives $\Omega_m = 0.252_{-0.150}^{+0.147}$ at 1σ confidence level with $\chi_{\text{min}}^2/N_{\text{d.o.f}} = 11.486$. The error bars have been obtained through the likelihood functions ($\mathcal{L} \propto e^{-\chi^2/2}$) marginalized over the nuisance parameter h . The likelihood functions for the four cases of (i) fitting model with Supernova data, (ii) combined analysis with the two experiments of SNIa+CMB, (iii) combined analysis with the three experiments of SNIa+CMB+SDSS and (iv) combining all four experiments of SNIa+CMB+SDSS+LSS are shown in Figures 5 and 6. The best fit value and age of universe computing in the $f(R)$ modified gravity model are reported in table II.

VI. AGE OF UNIVERSE

The age of universe integrated from the big bang up to now for flat universe in terms of X_0 is given by:

$$\begin{aligned} t_0(X_0) &= \int_0^{t_0} dt = \int_0^\infty \frac{dz}{(1+z)H(z)} \\ &= \frac{1}{3H_0} \int_{X_0}^\infty \frac{F' - XF''}{2F - XF'} \frac{dX}{\mathcal{H}(X)} \end{aligned} \quad (59)$$

Figure 7 shows the dependence of $H_0 t_0$ (Hubble parameter times the age of universe) on X_0 for a flat universe. In the lower panel we show it for Λ CDM for comparison. As we expect modified gravity behaves as a dark energy and increasing X_0 (Ω_λ) result in a longer age for the universe in the $f(R)$ modified gravity model.

The "age crisis" is one the main reasons of the acceleration phase of the universe. The problem is that the universe's age in the Cold Dark Matter (CDM) universe is less than the age of old stars in it. Studies on the old stars [53] suggest an age of 13_{-2}^{+4} Gyr for the universe. Richer et. al. [54] and Hasen et. al. [55] also proposed an age of 12.7 ± 0.7 Gyr, using the white dwarf cooling sequence method (for full review of the cosmic age see [5]). To do another consistency test, we compare the age of universe derived from this model with the age of old stars and Old High Redshift Galaxies (OHRG) in various redshifts. Table II shows that the age of universe from the combined analysis of SNIa+CMB+SDSS+LSS is $14.69_{-0.28}^{+0.29}$ Gyr and $13.61_{-0.15}^{+0.16}$ Gyr for new Gold sample and SNLS data, respectively. These values are in agreement with the age of old stars [53]. Here we take three OHRG for comparison with the power-law dark energy model, namely the LBDS 53W091, a 3.5-Gyr old radio galaxy at $z = 1.55$ [56], the LBDS 53W069 a 4.0-Gyr old radio galaxy at $z = 1.43$ [57] and a quasar, APM 08279 + 5255 at $z = 3.91$ with an age of $t = 2.1_{-0.1}^{+0.9}$ Gyr [58]. The latter has once again led to the "age crisis". An interesting point about this quasar is that it cannot

TABLE II. The best values for the parameters of $f(R)$ modified gravity with the corresponding age for the universe from fitting with SNIa from new Gold sample and SNLS data, SNIa+CMB, SNIa+CMB+SDSS and SNIa+CMB+SDSS+LSS experiments at one and two σ confidence level. The value of Ω_m was determined according to equation (19)

Observation	X_0	Ω_m	Age (Gyr)
SNIa(new Gold)	$6.207^{+0.230}_{-0.147}$	$0.276^{+0.376}_{-0.240}$	$14.71^{+0.41}_{-0.23}$
	$6.207^{+0.445}_{-0.515}$	$0.276^{+0.727}_{-0.276}$	$14.71^{+0.85}_{-0.75}$
SNIa(new Gold)+ CMB	$6.190^{+0.224}_{-0.242}$	$0.278^{+0.365}_{-0.278}$	$14.69^{+0.39}_{-0.37}$
	$6.190^{+0.433}_{-0.503}$	$0.278^{+0.706}_{-0.278}$	$14.69^{+0.82}_{-0.72}$
SNIa(new Gold)+ CMB+SDSS	$6.169^{+0.170}_{-0.184}$	$0.281^{+0.277}_{-0.281}$	$14.56^{+0.29}_{-0.28}$
	$6.169^{+0.327}_{-0.380}$	$0.281^{+0.533}_{-0.281}$	$14.56^{+0.58}_{-0.56}$
SNIa(new Gold)+ CMB+SDSS+LSS	$6.192^{+0.167}_{-0.177}$	$0.278^{+0.273}_{-0.278}$	$14.69^{+0.29}_{-0.28}$
	$6.192^{+0.321}_{-0.368}$	$0.278^{+0.524}_{-0.278}$	$14.69^{+0.55}_{-0.58}$
SNIa (SNLS)	$6.484^{+0.099}_{-0.099}$	$0.246^{+0.164}_{-0.164}$	$13.69^{+0.18}_{-0.17}$
	$6.484^{+0.196}_{-0.201}$	$0.246^{+0.324}_{-0.246}$	$13.69^{+0.37}_{-0.35}$
SNIa(SNLS)+ CMB	$6.477^{+0.098}_{-0.100}$	$0.246^{+0.162}_{-0.165}$	$13.68^{+0.18}_{-0.17}$
	$6.477^{+0.194}_{-0.200}$	$0.246^{+0.321}_{-0.246}$	$13.68^{+0.36}_{-0.33}$
SNIa(SNLS)+ CMB+SDSS	$6.428^{+0.090}_{-0.092}$	$0.252^{+0.148}_{-0.152}$	$13.60^{+0.16}_{-0.15}$
	$6.428^{+0.177}_{-0.185}$	$0.252^{+0.292}_{-0.252}$	$13.60^{+0.32}_{-0.30}$
SNIa(SNLS)+ CMB+SDSS+LSS	$6.433^{+0.089}_{-0.091}$	$0.252^{+0.147}_{-0.150}$	$13.61^{+0.16}_{-0.15}$
	$6.433^{+0.176}_{-0.183}$	$0.252^{+0.291}_{-0.252}$	$13.61^{+0.32}_{-0.30}$

TABLE III. The value of τ for three high redshift objects, using the parameters of the model derived from fitting with the observations at one and two σ level of confidences.

Observation	LBDS 53W069 $z = 1.43$	LBDS 53W091 $z = 1.55$	APM 08279 + 5255 $z = 3.91$
SNIa (new Gold)	$1.23^{+0.05}_{-0.03}$	$1.32^{+0.05}_{-0.03}$	$0.86^{+0.37}_{-0.05}$
	$1.23^{+0.10}_{-0.09}$	$1.32^{+0.11}_{-0.10}$	$0.86^{+0.38}_{-0.08}$
SNIa(new Gold)+CMB	$1.23^{+0.05}_{-0.04}$	$1.32^{+0.05}_{-0.05}$	$0.86^{+0.37}_{-0.06}$
	$1.23^{+0.10}_{-0.08}$	$1.32^{+0.11}_{-0.09}$	$0.86^{+0.38}_{-0.09}$
SNIa(new Gold)+CMB +SDSS	$1.23^{+0.03}_{-0.04}$	$1.32^{+0.04}_{-0.04}$	$0.85^{+0.36}_{-0.05}$
	$1.23^{+0.07}_{-0.06}$	$1.32^{+0.08}_{-0.07}$	$0.85^{+0.37}_{-0.07}$
SNIa(new Gold)+CMB +SDSS+LSS	$1.23^{+0.04}_{-0.03}$	$1.32^{+0.04}_{-0.04}$	$0.86^{+0.36}_{-0.05}$
	$1.23^{+0.07}_{-0.06}$	$1.32^{+0.08}_{-0.08}$	$0.86^{+0.37}_{-0.07}$
SNIa (SNLS)	$1.16^{+0.02}_{-0.02}$	$1.21^{+0.02}_{-0.02}$	$0.82^{+0.35}_{-0.04}$
	$1.16^{+0.02}_{-0.02}$	$1.21^{+0.02}_{-0.02}$	$0.82^{+0.35}_{-0.04}$
SNIa(SNLS)+CMB	$1.16^{+0.02}_{-0.02}$	$1.25^{+0.02}_{-0.02}$	$0.82^{+0.35}_{-0.02}$
	$1.16^{+0.05}_{-0.04}$	$1.25^{+0.05}_{-0.04}$	$0.82^{+0.36}_{-0.06}$
SNIa(SNLS)+CMB +SDSS	$1.15^{+0.02}_{-0.02}$	$1.24^{+0.03}_{-0.02}$	$0.81^{+0.35}_{-0.04}$
	$1.15^{+0.04}_{-0.04}$	$1.24^{+0.04}_{-0.04}$	$0.81^{+0.36}_{-0.05}$
SNIa(SNLS)+CMB +SDSS+LSS	$1.15^{+0.02}_{-0.02}$	$1.24^{+0.02}_{-0.02}$	$0.81^{+0.35}_{-0.04}$
	$1.15^{+0.04}_{-0.03}$	$1.24^{+0.04}_{-0.04}$	$0.81^{+0.36}_{-0.05}$

be accommodated in the Λ CDM model [59]. To quantify the age-consistency test we introduce the expression τ as:

$$\tau = \frac{t(z; X_0)}{t_{obs}} = \frac{t(z; X_0)H_0}{t_{obs}H_0}, \quad (60)$$

where $t(z)$ is the age of universe, obtained from the equation (59) and t_{obs} is an estimation for the age of old cosmological object. In order to have a compatible age for the universe we should have $\tau > 1$. Table III reports the value of τ for three mentioned OHRG with various observations. We see that $f(R)$ modified gravity with the parameters from the combined observations, provides a compatible age for the universe, compared to the age of old objects, while the SNLS data result in a shorter age for the universe. Once again, APM 08279 + 5255 at $z = 3.91$ has a longer age than the universe but gives better results than most cosmological models [60,61].

VII. CONCLUSION

Here in this work we obtained the dynamics of universe with $f(R) = \sqrt{R^2 - R_0^2}$ gravity and compared it with recent cosmological observations. This comparison has been performed with Supernova Type Ia Gold sample and SNLS supernova data, CMB shift parameter, location of baryonic acoustic oscillation peak observed by SDSS and large scale structure formation data by 2dFGRS. The best parameters obtained from fitting with the new Gold sample data are: $h = 0.63$, $X_0 = 6.192_{-0.177}^{+0.167}$ provides $\Omega_m = 0.278_{-0.278}^{+0.273}$ at 1σ confidence level with $\chi_{min}^2/N_{d.o.f} = 0.900$. Using the SNLS supernova data, the best fit value for model parameter is: $X_0 = 6.433_{-0.091}^{+0.089}$ gives $\Omega_m = 0.252_{-0.150}^{+0.147}$ at 1σ confidence level with $\chi_{min}^2/N_{d.o.f} = 11.486$. We also performed the age test, comparing the age of old stars and old high redshift galaxies with the age derived from this model. From the best fit parameters of the model using new Gold sample and SNLS, we obtained an age of $14.69_{-0.28}^{+0.29}$ Gyr and $13.61_{-0.15}^{+0.16}$ Gyr, respectively, for the universe which is in agreement with the age of old stars. We also chose two high redshift radio galaxies at $z = 1.55$ and $z = 1.43$ with a quasar at $z = 3.91$. The ages of the two first objects were consistent with the age of universe, means that they were younger than the universe while the third one was not.

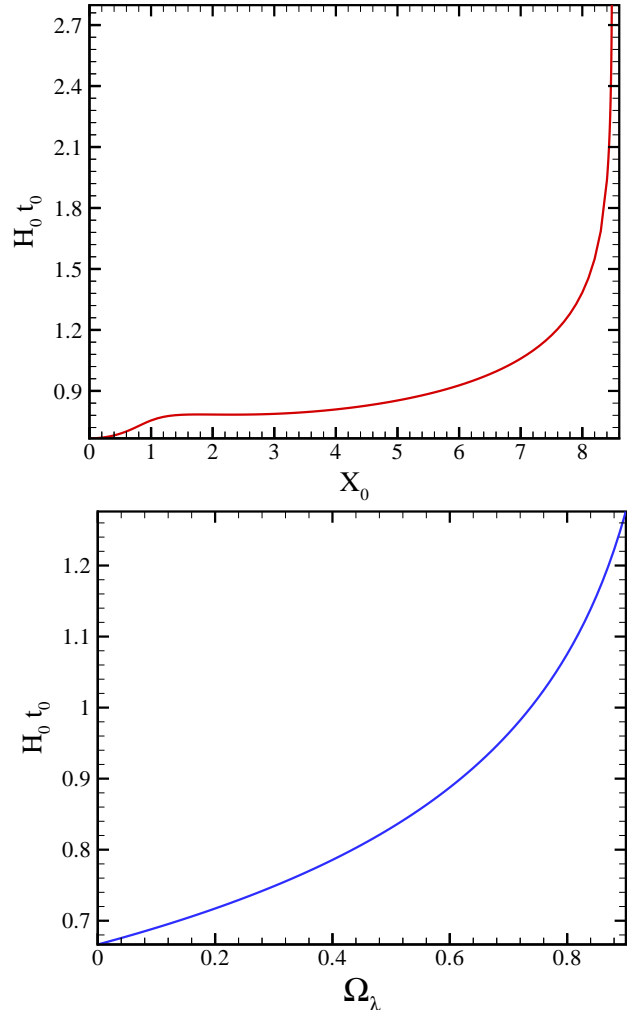


FIG. 7. $H_0 t_0$ (age of universe times the Hubble constant at the present time) as a function of $X_0 = R_0/H_0^2$ (upper panel). $H_0 t_0$ for Λ CDM versus Ω_λ (lower panel). Increasing X_0 gives a longer age for the universe. This behavior is the same as what happens in Λ CDM.

[1] A. G. Riess et al., *Astron. J.* **116**, 1009 (1998).
[2] S. Perlmutter et al., *Astrophys. J.* **517**, 565 (1999).
[3] C. L. Bennett et al., *Astrophys. J. Suppl. Ser.* **148**, 1 (2003).

[4] H.V. Peiris et al., *Astrophys. J. Suppl. Ser.* **148**, 213 (2003).
[5] D. N. Spergel, L. Verde, H. V. Peiris *et al.*, *Astrophys. J.* **148**, 175 (2003).
[6] S. Weinberg, *Rev. Mod. Phys.* **61**, 1 (1989); S. M. Carroll, *Living Rev. Relativity* **4**, 1 (2001); P. J. E. Peebles and B. Ratra, *Rev. Mod. Phys.* **75**, 559 (2003); T. Padmanabhan, *Phys. Rep.* **380**, 235 (2003).
[7] C. Wetterich, *Nucl. Phys. B* **302**, 668 (1988); P. J. E. Peebles and B. Ratra, *Astrophys. J.* **325**, L17 (1988); B. Ratra and P. J. E. Peebles, *Phys. Rev. D* **37**, 3406 (1988); J. A. Frieman, C. T. Hill, A. Stebbins, and I. Waga, *Phys. Rev. Lett.* **75**, 2077 (1995); M. S. Turner and M. White, *Phys. Rev. D* **56**, R4439 (1997); R. R. Caldwell, R. Dave, and P. J. Steinhardt, *Phys. Rev. Lett.* **80**, 1582 (1998); A. R. Liddle and R. J. Scherrer, *Phys. Rev. D* **59**, 023509 (1999); I. Zlatev, L. Wang, and P. J. Steinhardt, *Phys.*

- Rev. Lett. **82**, 896 (1999); P. J. Steinhardt, L. Wang, and I. Zlatev, Phys. Rev. D **59**, 123504 (1999); D. F. Torres, Phys. Rev. D **66**, 043522 (2002).
- [8] L. Amendola, Phys. Rev. D **62**, 043511 (2000); L. Amendola and D. Tocchini-Valentini, Phys. Rev. D **64**, 043509 (2001); **66**, 043528 (2002); L. Amendola, Mon. Not. R. Astron. Soc. **342**, 221 (2003); M. Pietroni, Phys. Rev. D **67**, 103523 (2003); D. Comelli, M. Pietroni, and A. Riotto, Phys. Lett. B **571**, 115 (2003); U. Franca and R. Rosenfeld, Phys. Rev. D **69**, 063517 (2004); X. Zhang, Phys. Lett. B **611**, 1 (2005).
- [9] P. J. E. Peebles, R. Ratra, Astrophys. J. **325**, L17 (1988).
- [10] C. Armendariz-Picon, V. Mukhanov and P. J. Steinhardt, Phys. Rev. Lett. **85**, 4438 (2000).
- [11] J. S. Bagla, H. K. Jassal and T. Padmanabhan, Phys. Rev. D **67**, 063504 (2003).
- [12] R. R. Caldwell, Phys. Lett. B **545**, 23 (2002).
- [13] R. R. Caldwell, M. Kamionkowski and N. N. Weinberg, Phys. Rev. Lett. **91**, 071301 (2003).
- [14] A. Kamenshchik, U. Moschella and V. Pasquier, Phys. Lett. B **511**, 265 (2001).
- [15] S. Arbabi Bidgoli, M. S. Movahed, and S. Rahvar, Int. J. Mod. Phys. D **15**, 1455 (2006).
- [16] L. Wang, R. R. Caldwell, J. P. Ostriker and P. J. Steinhardt, Astrophys. J. **530**, 17 (2000).
- [17] S. Perlmutter, M. S. Turner and M. White, Phys. Rev. Lett. **83**, 670 (1999).
- [18] L. Page *et al.*, Astrophys. Supp. J. **148**, 233 (2003).
- [19] M. Doran, M. Lilley, J. Schwindt and C. Wetterich, Astrophys. J. **559**, 501 (2001).
- [20] M. Doran, M. Lilley, Mon. Not. Roy. A. Soc. **330**, 965 (2002).
- [21] R. R. Caldwell and M. Doran, Phys. Rev. D **69**, 103517 (2004).
- [22] S. Nojiri and S. D. Odintsov, Gen. Rel. Grav. **36**, 1765 (2004); M. E. Soussa and R. P. Woodard, Gen. Rel. Grav. **36**, 855 (2004); G. Allemandi, A. Borowiec and M. Francaviglia, Phys. Rev. D **70**, 103503 (2004); D. A. Easson, Int. J. Mod. Phys. A **19**, 5343 (2004); S. M. Carroll, A. De Felice, V. Duvvuri, D. A. Easson, M. Trodden and M. S. Turner, Phys. Rev. D **71**, 063513 (2005); S. Carloni, P. K. S. Dunsby, S. Capozziello and A. Troisi, Class. Quant. Grav. **22**, 4839 (2005); S. Capozziello, V. F. Cardone and A. Troisi, Phys. Rev. D **71**, 043503 (2005); G. Cognola, E. Elizalde, S. Nojiri, S. D. Odintsov and S. Zerbini, JCAP **0502**, 010 (2005); S. Nojiri, S. D. Odintsov and S. Tsujikawa, Phys. Rev. D **71**, 063004 (2005); T. Clifton and J. D. Barrow, Phys. Rev. D **72**, 103005 (2005); S. Das, N. Banerjee and N. Dadhich, Class. Quant. Grav. **23**, 4159 (2006); S. Capozziello, V. F. Cardone, E. Elizalde, S. Nojiri and S. D. Odintsov, Phys. Rev. D **73**, 043512 (2006); T. P. Sotiriou, Class. Quant. Grav. **23**, 5117 (2006); A. De Felice, M. Hindmarsh and M. Trodden, JCAP **0608**, 005 (2006); S. Nojiri and S. D. Odintsov, Phys. Rev. D **74**, 086005 (2006); A. F. Zakharov, A. A. Nucita, F. De Paolis and G. Ingrosso, Phys. Rev. D **74**, 107101 (2006); P. Zhang, Phys. Rev. D **73**, 123504 (2006); K. Atazadeh and H. R. Sepangi, arXiv:gr-qc/0602028; S. M. Carroll, I. Sawicki, A. Silvestri and M. Trodden, arXiv:astro-ph/0607458; D. Huterer and E. V. Linder, arXiv:astro-ph/0608681; X. h. Jin, D. j. Liu and X. z. Li, arXiv:astro-ph/0610854; N. J. Poplawski, arXiv:gr-qc/0610133; V. Faraoni, arXiv:astro-ph/0610734; Y. S. Song, W. Hu and I. Sawicki, arXiv:astro-ph/0610532; I. Navarro and K. Van Acoleyen, arXiv:gr-qc/061112; R. Bean, D. Bernat, L. Pogosian, A. Silvestri and M. Trodden, arXiv:astro-ph/0611321; T. Chiba, T. L. Smith and A. L. Erickcek, arXiv:astro-ph/0611867; V. Faraoni and S. Nadeau, arXiv:gr-qc/0612075; E. O. Kahya and V. K. Onemli, arXiv:gr-qc/0612026;
- [23] S. Rahvar and Y. Sobouti, arXiv:0704.0680
- [24] S. Baghran, M. Farhang and S. Rahvar Phys. Rev. D **75**, 044024 (2007)
- [25] A. Melchiorri, L. Mersini, C.L. Ödman and M. Trodden, arXiv:astro-ph/0211522.
- [26] W. L. Freedman *et al.*, Astrophys. J. Lett. **553**, 47 (2001).
- [27] X. Zhang and F.Q. Wu, Phys. Rev. D **72**, 043524 (2005)
- [28] V. V. Nesterenko, Phys. Rev. D **75**, 087703 (2007)
- [29] G. Allemandi, A. Borowiec and M. Francaviglia, Phys. Rev. D. **70**, 043524 (2004); G. Allemandi, A. Borowiec and M. Francaviglia, Phys. Rev. D. **70**, 103503 (2004); M. Amarguioui, O. Elgaroy, D.F. Mota, T. Multamaki, A&A **454** 707 (2006); T. P. Sotiriou and S. Liberati, Annals Phys. **322** 935 (2007)
- [30] B. P. Schmidt *et al.*, Astrophys. J. **507**, 46 (1998).
- [31] A. G. Riess *et al.*, Astrophys. J. **607**, 665 (2004).
- [32] J. L. Tonry *et al.*, Astrophys. J. **594**, 1 (2003).
- [33] B. J. Barris *et al.*, Astrophys. J. **602**, 571 (2004).
- [34] The Gold dataset is available at <http://braeburn.pha.jhu.edu/ariess/R06>.
- [35] P. Astier *et al.*, astro-ph/0510447.
- [36] H. K. Jassal *et al.*, astro-ph/0601389.
- [37] S. Nesseris and L. Perivolaropoulos, Phys. Rev. D **70**, 043531 (2004).
- [38] Hu, W., Sugiyama, N., Silk, J., Nat, 386, **37** (1997)
- [39] W. Hu and N. Sugiyama, Astrophys. J. **444**, 489 (1995).
- [40] W. Hu, M. Fukugita, M. Zaldarriaga and M. Tegmark, Astrophys. J. **549**, 669 (2001)
- [41] M. Doran and M. Lilley, Mon. Not. R. Astron. Soc. **330**, 965 (2002)
- [42] J. R. Bond, G. Efstathiou, and M. Tegmark, Mon. Not. R. Astron. Soc. **291**, L33 (1997); A. Melchiorri, L. Mersini, C. J. Odman, and M. Trodden, Phys. Rev. D **68**, 043509 (2003); C. J. Odman, A. Melchiorri, M. P. Hobson, and A. N. Lasenby, Phys. Rev. D **67**, 083511 (2003).
- [43] T. J. Pearson *et al.* (CBI Collaboration), Astrophys. J. **591**, 556 (2003); C. L. Kuo *et al.* (ACBAR Collaboration), Astrophys. J. **600**, 32 (2004).
- [44] D. J. Eisenstein *et al.*, Astrophys. J. **633** 441 (2005)
- [45] C. L. Bennett, R. S. Hill and G. Hinshaw, Astrophys. J. Suppl. **148**, 97 (2003).
- [46] Padmanabhan T., 1993, Structure Formation in the Universe. Cambridge Univ. Press
- [47] Brandenberger, R. H., 2004, in Breton N., Cervantes-Cota J. L., and Salgado, M., eds, Lecture Notes in Physics, , The early universe and observational cosmology, 646, p.127
- [48] K. Koyama and R. Maartens, JCAP **0601**, 016 (2006),
- [49] Peebles, P. J. E., 1980, The Large Scale Structure of the Universe, Princeton University Press, Princeton, NJ

- [50] Mansouri, R., Rahvar, S, 2002, *Int. J. Modern Phys. D*, **11**, 312
- [51] Verde L., Kamionkowski M., Mohr J. J., Benson A.J., 2001, *MNRAS*, **321**, L7
- [52] Lahav O., Bridle S. L., Percival W. J., & the 2dFGRS Team, 2002, *MNRAS*, **333**, 961
- [53] E. Carretta et al., *Astrophys. J.* **533**, 215 (2000); B. Chaboyer and L. M. Krauss, *Astrophys. J. Lett.* **567**, L45 (2002).
- [54] H. B. Richer et al., *Astrophys. J.* **574**, L151 (2002).
- [55] B. M. S. Hansen et al., *Astrophys. J.* **574**, L155 (2002).
- [56] J. Dunlop et. al., *Nature (London)* **381**, 581 (1996); H. Spinrard, *Astrophys. J.* **484**, 581 (1997).
- [57] J. Dunlop, in *The Most Distant Radio Galaxies*, edited by H. J. A. Rottgering, P. Best, and M. D. Lehnert (Kluwer, Dordrecht, 1999), p. 71.
- [58] G. Hasinger, N. Scharrel and S. Komossa, *Astrophys. J. Lett.* **573**, L77 (2002)
- [59] D. Jain., A. Dev., *Phys. Lett. B* **633** (2006) 436
- [60] M. Sadegh Movahed and S. Rahvar, *Phys.Rev. D* **73** (2006) 083518.
- [61] S. Rahvar and M. Sadegh Movahed, *Phys. Rev. D* **75** (2007) 023512.